Hall effect evidence for an interplay between electronic correlations and Na order induced electronic bands topology in Na_xCoO_2

I. F. Gilmutdinov [1,*] I. R. Mukhamedshin [1,2] and H. Alloul [2]
[1]*Institute of Physics, Kazan Federal University, 420008 Kazan, Russia*
[2]*Université Paris-Saclay, CNRS, Laboratoire de Physique des Solides, 91405 Orsay, France*

(Received 24 January 2020; accepted 17 March 2020; published 16 April 2020)

The incidence of topology on the band structure and physical properties of layered compounds has been extensively studied in semimetals. How those evolve in the presence of electronic correlations has been less investigated so far. In the sodium cobaltates Na_xCoO_2 considered here, unexpected magnetic properties associated with correlations on the Co sites were disclosed about 15 years ago. It has also been found that various orderings of the Na atoms occur in between the CoO_2 layers in the stable phases of these cobaltates. The distinct Na orders of these phases have been shown to induce specific Co charge disproportionation with large-size unit cells in the CoO_2 planes, linked with the diverse magnetic behaviors. This provides an original playground in the studies of interplays between topology and correlations in these layered materials. We present here transport measurements on a series of single crystals and demonstrate that we do synthetize pure phases with quite reproducible transport properties. We show that above room temperature those display a similar behavior whatever the Na content. On the contrary, we provide evidence for a great diversity in Hall effect low-temperature dependences which underscores the specificities of the Fermi-surface reconstructions induced by the Na order. We study in some detail the difference between two metallic phases, one ($x = 0.77$) antiferromagnetic below $T_N = 22$ K and the second ($x = 2/3$) paramagnetic down to $T = 0$. Both show a sign change in the Hall effect with decreasing T. We demonstrate that this can be attributed to quite distinct physical effects. For the $x = 0.77$ phase the negative Hall effect has a nonlinear field dependence and occurs in similar conditions to the anomalous Hall effect found in various magnetic metals. In the $x = 2/3$ phase in which the Co sites are disproportionated in a kagome substructure, the negative sign of the Hall effect and its two-step T variation have to be assigned to specificities of its Fermi surface. In both cases the anomalies detected in the Hall effect are certainly associated with the topology of their Co electronic bands.

DOI: 10.1103/PhysRevMaterials.4.044201

I. INTRODUCTION

A great evolution in the physical studies of layered metals has occurred in the last 30 years. The discovery of high-T_C superconductivity (SC) in cuprates has been at the origin of many research activities on transition-metal oxide materials. The importance of electronic correlations (EC) on the Cu sites has been underlined by the existence of their magnetic properties [1]. Studies on other transition-metal compounds have been mostly motivated by the search for unconventional SC properties. For instance a special attention has been devoted to the cobaltates Na_xCoO_2 after the discovery of SC with $T_C \sim 5$ K in a hydrated phase for $x \approx 0.3$ [2]. In these compounds the Co sites form a triangular two-dimensional (2D) lattice, and magnetism was unexpectedly found to occur for $x > 0.7$ [3,4]. The interest in these compounds faded away, as SC has not been found so far in nonhydrated compounds.

Later on the discovery of the properties of the graphene layer [5] with Dirac cones in its band structure [6] has aroused a great interest in materials for which the electronic bands involve singular points protected by their topology [7]. Specific materials often with unit cells without inversion symmetry have been shown to exhibit such singular Dirac or Weyl [8] points (the latter occur above or below the Fermi level). Those have been initially evidenced in materials with weak electronic correlations, as is the case for the single-layer graphene. But nowadays it has become clear that such topological properties might occur as well in materials with strong EC and can yield original magnetic properties which might become useful in spintronics applications. There is therefore a growing interest in correlated electron compounds in which topological effects might occur.

Coming back to the cobaltates which are clearly correlated electron systems, their triangular lattice structure differentiates them from the nearly square lattice cuprate structure. Furthermore, nuclear magnetic and quadrupolar resonance (NMR/NQR) experiments on aligned powder samples disclosed a series of Na ordered phases [9] also seen by transmission electron microscopy [10]. The local spin susceptibilities measured by the Co NMR shift revealed specific disproportionations of the Co charges with singular large-size unit cells in the CoO_2 layers. For instance, a kagome Co sublattice has been shown to exist for $x = 2/3$ [11,12]. We thus point out that EC and topological states are concomitant in these materials. This emphasizes the interest to consider in some

*ildar.gilmutdinov@gmail.com; present address: Laboratoire National des Champs Magnétiques Intenses, 31400 Toulouse (France).

detail the influence of the charge order on the Co sites on the physical properties in real and k spaces.

So far the sodium cobaltates have been found metallic for nearly any Na content. But the initial experiments did not reveal a clear picture of the actual evolution of the band structure with the Na concentration. Calculations within a local density approximation (LDA) ignoring the Na order do not reproduce the charge differentiation. They imply a large hexagonal 2D Fermi surface (FS) with eventually some small pockets for low Na doping [13,14]. Those results were apparently partly supported by angle-resolved photoemission spectroscopy data (ARPES), although small pockets were never observed [15]. On the contrary, the quantum oscillations (QO) detected in initial transport measurements imply the existence of small carrier pockets in the ground state [16].

Some care has to be exercised in the analyses of those initial experiments. ARPES is a technique which probes surface states. After cleaving the samples between CoO_2 planes in the *ab* direction, the average Na content left on the top layer should be $x/2$ in order to satisfy charge neutrality. This cannot maintain the same ordered state of the Co planes as the bulk. On the contrary, transport experiments are quite sensitive to the Fermi-surface reconstructions induced by the Co charge order in the bulk single crystals. But in that respect, so far the main difficulty has been the production of homogeneous and reproducible single crystals. Recently we have made specific efforts to control as much as possible the quality of single-crystal samples of ordered Na phases [17]. This enables us now to probe the bulk electronic properties by resistivity and Hall effect measurements. The high quality of our samples is reflected by the large differences found between the various ordered phases and by the reproducibility of our data. Here we specifically study the T and applied magnetic field B dependences of the Hall effect, which is currently a good probe of unusual incidences of the topology on the band structure of metals and semimetals.

The paper is organized along the following line. We first display in Sec. II the large differences in transport we observed on a series of well-controlled ordered Na phases. This permits us to reveal in many cases sign changes of the Hall effect, which evidences that the Co disproportionation induced by the Na order induces a multiband character. We then select two phases which apparently display at low T similar large negative values of the Hall constant. In Sec. III we demonstrate that in the $x = 0.77$ phase [18] this behavior is connected with the establishment of an ordered metallic antiferromagnetic (AF) state at low T. On the contrary, we show in Sec. IV that for the $x = 2/3$ phase [11] the sign change of the Hall effect occurs in a purely paramagnetic state and must be associated with the specific band structure of this phase. A rough quantitative analysis of the Hall effect performed in Sec. V leads us to suggest that a single-band picture might apply for the AF phase, while multiband behavior is required to explain the Hall effect in the $x = 2/3$ phase. We also discuss the possible analogies of the anomalous behavior of the Hall effect (AHE) compared to that seen in various magnetic metals. Similarly, we consider the possible relation between the Hall anomalies seen in the $x = 2/3$ compound and its reconstructed kagome band structure.

II. COMPARISON OF TRANSPORT PROPERTIES OF DIFFERENT PHASES

We have performed transport measurements with the standard techniques detailed in Appendix A. The longitudinal resistance R_{xx} and the transverse resistance R_{xy} measured in an applied field B give respective measures of the resistivity ρ and of the Hall constant R_H after taking into account the geometrical factors of the sample. Data have been taken on single crystals of five phases which had been singled out using powder samples [19]. The distinct Na orders revealed by NMR in some of these phases are illustrated in Fig. 1(a). We found that some characteristics of the resistivity and Hall effect data were perceptible in the initial papers [20].

Resistivity data. As can be seen in the upper part of Fig. 1(b), all pure phases were found to display metallic resistivity except that for $x = 1/2$. This phase had been identified early on and is known to exhibit a magnetic transition at 86 K [21,22] not detected by transport techniques and a metal-insulator transition at $T \approx 51$–53 K [23]. The latter is clearly seen in Fig. 1(c), in which a secondary increase of ρ is seen to occur below 20 K so that the resistivity increases by a factor of $\sim$100 from 50 K to low T.

For the other phases we measured in our single crystals residual resistivities ρ_0 much lower than those found in former publications (with resistivity ratios as high as a few hundred given in Appendix A). The ρ_0 values and the differences in the quoted Na content indicate that the samples studied in the early papers were quite often mixtures of Na ordered phases [20].

For all phases, the high-T behaviors of $\rho(T)$ are found to be quite similar, as can be seen in the upper part of Fig. 1(b). The actual differences in $\rho(T)$ for these phases are mostly seen at low T on the resistivity derivatives $d\rho/dT$, as will be displayed in the following sections.

Hall effect. In these five phases the T dependence of the Hall effect has been found to display major differences. The Hall constant R_H is seen in the lower part of Fig. 1(b) to become negative in most cases at low temperature. Such a behavior is totally unexpected within the framework used to analyze the initial experiments and suggests that the Fermi surface is temperature dependent. The $x = 1$ parent phase has been established as being a band insulator involving only Co^{3+} states in which the t_{2g} sublevels are filled [24,25]. From LDA band structure calculations one expects a progressive depletion of these levels with decreasing x. This continuous increase of hole carrier density due to Na vacancy doping is apparently seen for the surface states probed by ARPES measurements [15]. One would then expect a temperature-independent positive Hall effect for any Na content. This is never seen to happen in our set of data, although a positive Hall effect is always seen above room temperature. The large decrease of the Hall effect and its sign changes which occur with decreasing T clearly demonstrate that the simple LDA picture does not apply for the planar ordered electronic states.

The negative Hall effect regimes reveal the occurrence of carrier bands with a dominant electronic character and imply that the Na order has induced a Fermi-surface reconstruction. This is somewhat similar to the observations done in the

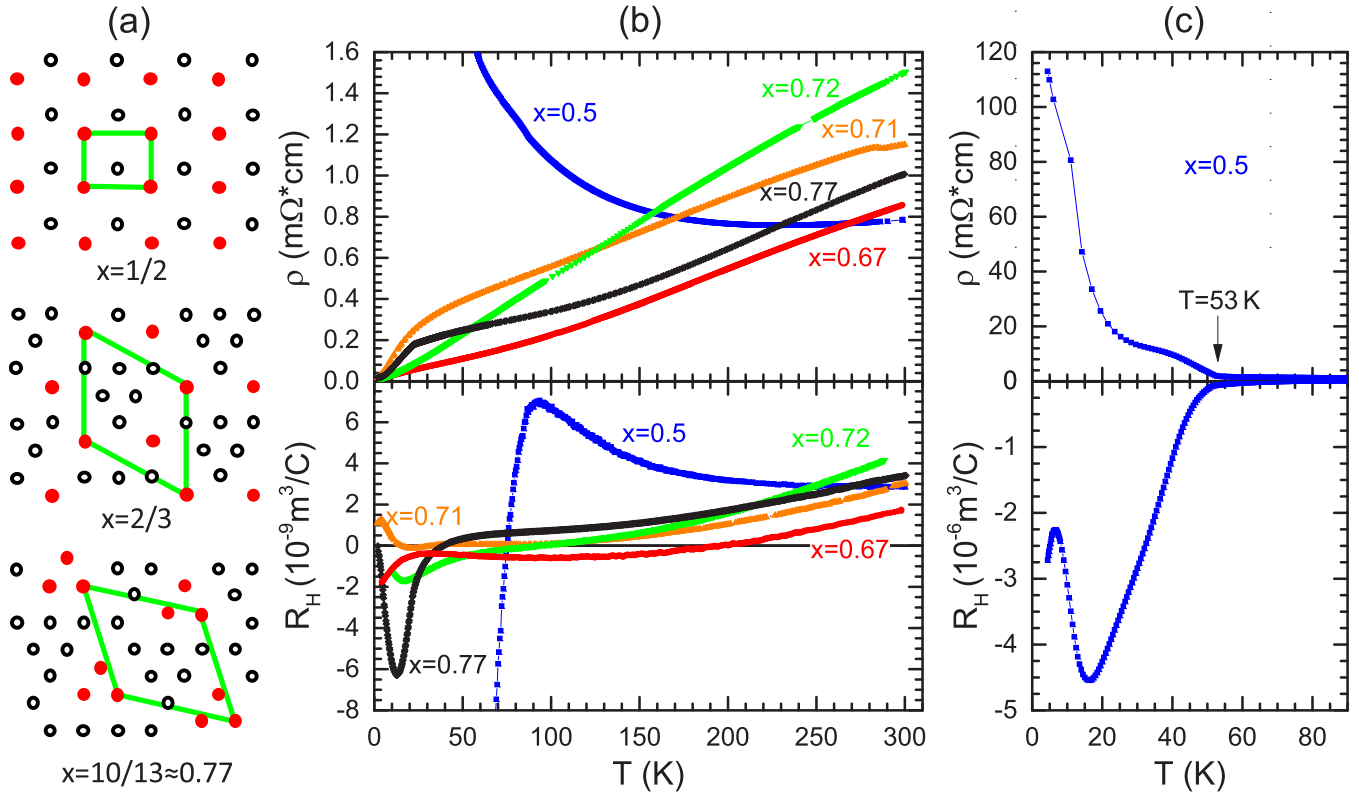

FIG. 1. (a) Three typical Na ordered phases. Here the Co atoms located on the triangular lattice sites are not represented. The Na atoms are located either on top of a Co site (red) or on top of a triangle of Co atoms (black) [9]. (b) Zero field resistivity and Hall constant data measured in a 9-T applied field (respectively in the upper and lower frames) for five typical phases. They differ markedly at low temperatures (see text). (c) The low-T data for the $x = 1/2$ phase are displayed on enlarged scales. This underlines the metal-to-"insulator" transition at 53 K.

underdoped cuprate pseudogap regime [26]. This analogy with the present results is then in line with the early detection in the cobaltates of QO due to small Fermi pockets [16] prior to the discovery of QO in the cuprates [27]. The NMR [9] and x-ray [12] experiments have given evidence that the Na atomic order is already established at room temperature, so the low-temperature Hall data are certainly due to fine effects of the reconstructed FS topology.

Above room temperature the positive Hall effect measured in all samples apparently implies that in that temperature range the transport properties are governed by hole carriers. On the other hand, R_H is seen to increase regularly with increasing T around room temperature in all samples. This behavior was clearly noticed even up to much higher T in the initial experiments on a given sample [28]. Such a linear increase of the Hall effect has indeed been suggested to be a specific behavior for uniformly doped triangular metallic lattices, whatever the doping and EC strength [29,30]. The present results do generally support this theoretical suggestion.

The main idea is that this effect is associated with thermal shifts of the chemical potential. A similar suggestion had been proposed from transport [31] experiments in Fe pnictides and supported by ARPES experiments [32], although the origins of the shift of chemical potential are quite distinct in those compounds. Here it is mainly associated with the triangular structure of the lattice. Let us notice that this temperature variation is specifically seen in the regime for which Na diffusion and ionic conductivity becomes significant. Does that induce a situation similar to that which prevails for the ARPES data taken on disordered surface states? That could mean that the transport properties above room temperature become insensitive to the Na order induced reconstruction of the FS. We notice, however, that R_H does not evolve regularly with decreasing x at a given T, which could mean that local Na order still has an influence on the slope of the high-T variation of R_H.

In any case, the sign changes of the Hall effect in the lower part of Fig. 1(b) are always found to occur below room temperature, where the Na order and charge differentiation are already fully established. This happens together with the onset of anomalous magnetic responses that signal the importance of electronic correlations.

The $x = 0.77$ phase which develops an ordered magnetism below $T_N = 22$ K has a positive Hall effect down to low $T \sim 50$ K. But it becomes large and negative when T approaches T_N and *apparently recovers a nearly null value at* $T = 0$ [see bottom of Fig. 1(b)]. On the contrary, for $x = 2/3$ the Hall effect becomes negative for $T < 200$ K. The magnitude of the Hall effect increases then down to $T = 0$ in two steps in this peculiar phase in which a disproportionated state with a kagomelike structure occurs. The clearcut difference between these phases justifies our first-step choice to investigate the actual origin of these distinctly singular behaviors.

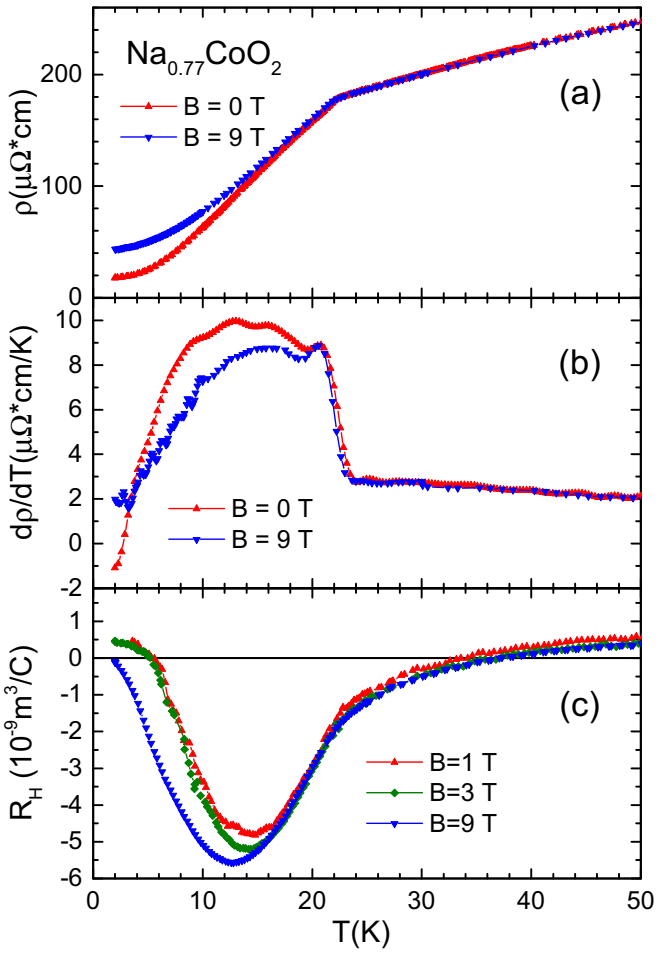

FIG. 2. (a) In any applied field the resistivity of the $x = 0.77$ phase drops below $T_N = 22$ K. A quite large positive magnetoresistance appears below T_N. (b) The abrupt increase of the derivative of the resistivity at T_N illustrates the sharpness of the AF transition. (c) The Hall constant measured for $B = 9$ T is small and positive at high temperatures but progressively becomes large and negative already above T_N. For a lower applied field a pronounced variation of R_H with B is seen below about 15 K.

III. AF PHASE WITH $x = 0.77$

Let us consider the most concentrated Na phase which exhibits a definite AF order. In most previous magnetic studies it has been found that an A-type AF order is established for most phases with $x > 0.75$ [33]. This corresponds to Co ferromagnetic layers with moments in the c direction which alternate in magnetic orientation from layer to layer.

The AF transition is perfectly apparent in the transport properties, as a sharp drop of $\rho(T)$ occurs at $T_N = 22$ K [Fig. 2(a)]. This is very clear with $d\rho/dT$ [Fig. 2(b)] and quite reproducible, as can be seen in Appendix B. The resistivity above T_N is therefore associated with a large magnetic scattering contribution in the paramagnetic (PM) state, which is quenched when the magnetization freezes so that a very good metallicity is restored in the low-temperature state. We also see there that the magnetoresistance (MR) is positive and large ($\approx$100%) at $T \ll T_N$ and becomes quite negligible in the PM state.

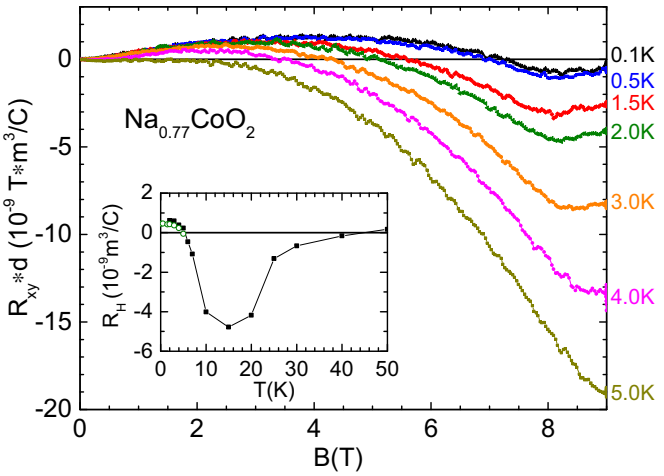

FIG. 3. The field dependence of the Hall effect illustrated here below $T = 5$ K gives evidence for two competing contributions. In the inset the linear contribution to the Hall effect extracted from the initial slope is plotted vs temperature. This has been done independently for two samples (empty green circles from the present data and filled squares from the data shown in Appendix C, taken above 2 K in a PPMS on a distinct sample).

As for the Hall effect, as can be seen in the lower half of Fig. 1(b), it has a behavior quite distinct from that observed in most other phases. First, it remains *positive* down to 50 K, which is a much lower temperature than in the other phases. Below 50 K it becomes negative and goes through a large maximum in absolute value at around 15 K, which is found to be quite reproducible (Appendix B). Finally R_H decreases towards zero at low T, as emphasized in the low-T plot of Fig. 2(c), which is somewhat unique when compared to the other phases. However, we noticed, as shown there, that the Hall constant also exhibits an unexpected field dependence below about 15 K.

The fact that the Hall voltage becomes nonlinear with the applied field B could be better seen in the data taken at fixed T versus B presented in Fig. 3. We clearly see there that the Hall effect even changes sign with applied field at low T. The simplest analysis of these data can be done by extracting the initial linear in-field contribution. The latter is found to be positive at the lowest temperature $T \ll T_N$. But for increasing T this positive contribution is overwhelmed by a negative term which has a more complex T and B dependence. Finally, as can be seen in Appendix C on the data taken in a physical properties measurement system (PPMS), the nonlinearity of the field dependence of this negative contribution decreases markedly with increasing temperatures above 15 K so that R_H becomes field independent above $T_N = 22$ K.

We also evidence at low temperature a kink in the Hall effect at about 8 T (on both Figs. 3 and 8 in Appendix C) which we could associate with a steplike increase seen at the same field on the magnetization (Fig. 9 in Appendix D). This reveals a spin flop or a metamagnetic transition. Therefore all these results clearly evidence that the magnetism has an influence on the scattering of the carriers and induces a magnetoresistance. Such effects appear even above T_N, while the static magnetic order is not established and could still

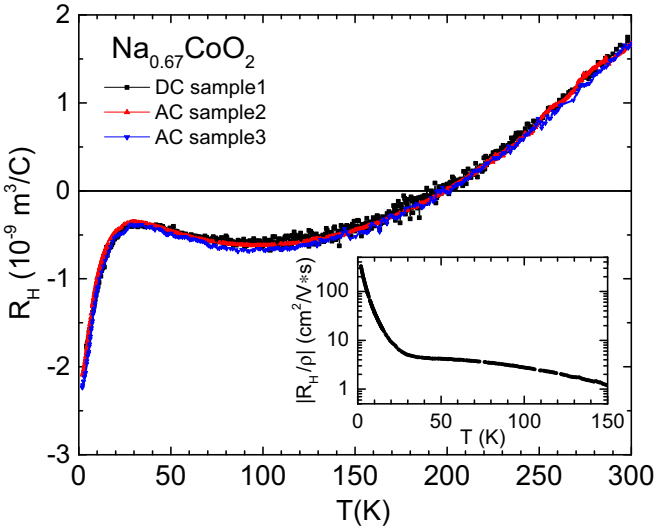

FIG. 4. Hall constant for the $x = 2/3$ phase taken in an applied field $B = 9$ T in distinct experimental setups using AC or DC current excitations (see Appendix A). The change of sign of the Hall effect at 200 K and the minimum in its absolute value at 30 K are found to be quite reproducible. In the inset the ratio $|R_H/\rho|$, which would correspond the electron mobility in the single-band model discussed in Sec. V, is reported up to 150 K.

be connected with the appearance of a dynamic short-range 2D ferromagnetic order. Such anomalous contributions to the Hall effect are commonly detected nowadays in diverse metallic magnetic materials and are associated with quite distinct possible origins, as discussed later in Sec. V. In the $x = 0.77$ phase this contribution apparently disappears in the $T = 0$ limit at low fields so that the positive linear term might be associated *with the normal Hall contribution of the free carriers*.

IV. $x = 2/3$ KAGOMELIKE PHASE

Let us now consider the $x = 2/3$ phase in which the charge disproportionation has been studied thoroughly by

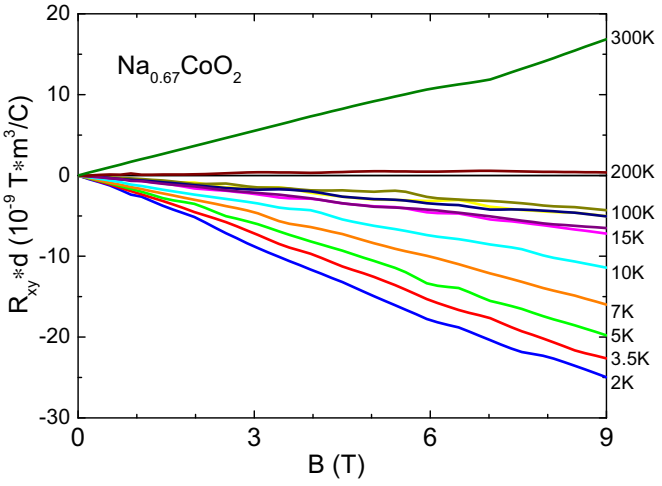

FIG. 5. Field dependence of R_{xy} in an $x = 2/3$ sample taken in a PPMS. The linear fits of these data have been used to derive the R_H values reported in the inset of Fig. 3.

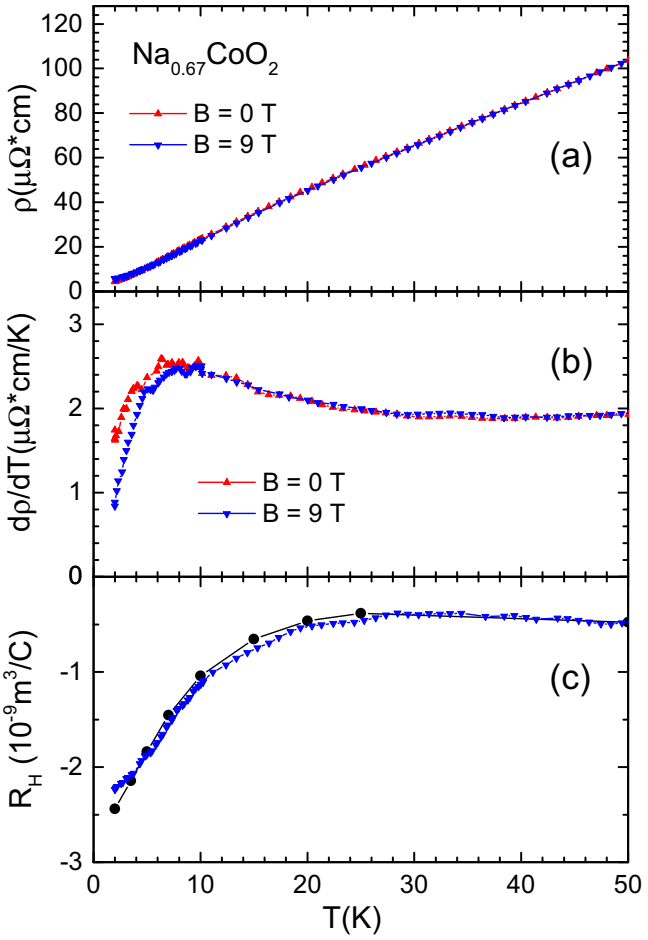

FIG. 6. The low-T data measured in zero field for ρ in (a) and $d\rho/dT$ in (b) are compared to those measured for $B = 9$ T. It can be seen that the magnetoresistance remains quite small. The Hall coefficient R_H data measured at 9 T on sample 3 of Fig. 4 are plotted in (c). They display a minimum in absolute value, which coincides with the decrease of $d\rho/dT$. These R_H data agree perfectly with those (full circles) obtained on a distinct sample, as deduced from the linear field dependence of the Hall voltage data shown in Fig. 5.

NMR/NQR experiments which revealed a kagome sublattice of Co sites [11,12]. In this phase a large regular decrease of $\rho(T)$ is observed, with the smallest residual resistivity found in our five phases, as can be seen in Fig. 1(b) and in Appendix A. Here again the Hall effect plotted in the lower part of Fig. 1(b) is positive at room temperature, as for the other phases, but it already becomes negative below 200 K. This sign change was found to be quite reproducible on many samples, as can be seen in Fig. 4.

At even lower temperatures of about 40 K, *a second reproducible Hall effect anomaly is detected*. Contrary to the case of the $x = 0.77$ phase, R_H remains negative and even increases in absolute value down to the lowest temperatures. Furthermore, the Hall voltage is found to be linear in fields down to the lowest temperature, as displayed in Fig. 5.

If one compares the behavior of the Hall effect with that of resistivity, one can see in Fig. 6 that the onset of the low-T decrease of the Hall effect coincides with the onset of a decrease of $d\rho/dT$, which indicates an inflection point at

about 30 K which is also found to be quite reproducible [17]. We might notice as well that the change of behavior of the Hall effect is concomitant with the large increase of the spin susceptibility detected by NMR without any onset of magnetic order down to $T = 0$ [34].

At odds with the $x = 0.77$ data, the resistivity for $B||c$ does not differ markedly from that measured in zero field. So the magnetoresistance remains small in all the temperature ranges considered. The large negative contribution to the Hall effect also behaves qualitatively quite differently than for $x = 0.77$. All these facts suggest that the strange behavior of the temperature variation of the Hall effect is linked with narrow features in the metallic band structure and not with the appearance of a magnetic order.

V. DISCUSSION

We have seen that the negative contribution to the Hall effect seen in the $x = 0.77$ phase appears to be connected with an AHE contribution associated with the magnetic response in the metallic state. Otherwise, the normal carrier band contribution to the Hall effect is positive for the $x = 0.77$ phase and negative for the $x = 2/3$ phase. That essentially means that the carriers which dominate the transport properties are holes in the former case and electrons in the latter. Let us consider first the possible origin of these normal contributions to the Hall effect.

A. Normal charge contribution to the Hall effect

An analysis of the transport properties can be carried out when the Fermi surface is known either by ARPES or at least from LDA calculations, as could be done in the case of iron pnictides [31]. In such cases for which the FS presents multiple bands and 2D cylindrical carrier pockets with both electronic and hole character, the dominant charge carriers were found to be somewhat dependent on doping [35]. In the present case, as pointed out in the Introduction, the reconstructed FS is not known so far, and at the moment we can only consider rough models. The simplest one is to assume two types of carriers with respective hole and electron content n_h and n_e and mobility μ_h and μ_e. In such a case [31,35],

$$\sigma = \rho^{-1} = n_h e\mu_h + n_e e\mu_e, \tag{1}$$

and

$$R_H\sigma^2 = \left[n_h e{\mu_h}^2 - n_e e{\mu_e}^2\right]. \tag{2}$$

In the $x = 0.77$ phase the leading contribution to $R_{\rm H}$ at $T = 0$ in low applied field has a magnitude $R_{\rm H} \approx 0.5 \times 10^{-9}\,{\rm m}^3/{\rm C}$, which is rather close to that found at about 50 K in the PM state (inset of Fig. 3). One might then speculate that the normal-state positive Hall effect would be temperature independent below about 50 K in the absence of ordered magnetism. One may even assume that a single-band model might apply with $n_e = 0$, which would be compatible with the very small magnetoresistance found experimentally. In such an oversimplified model the mobility would be given by $\mu_h = R_{\rm H}/\rho$, that is, $\mu_h \approx 28\,{\rm cm}^2/({\rm V\,s})$ at $T = 2\,{\rm K}$. This model would result in a nearly temperature-independent hole content $n_h = (R_{\rm H}e)^{-1} = 0.47/{\rm Co}$. Notice that this value is twice as large as the 0.23/Co value expected for a homogeneous doping of the CoO_2 planes but would better agree with the disproportionated state value described by the NMR data in this phase [36].

For the $x = 2/3$ phase, $R_{\rm H}$ is always negative below 200 K but displays a singular low-temperature variation. Both hole and electron carrier bands are required. But even if we do apply the charge neutrality condition $n_h - n_e = 1 - x$, we cannot deduce three parameters (n_e, μ_h, and μ_e) with the two observables given by Eqs. (1) and (2). We may, however, again oversimplify the problem by assuming that $\mu_h \ll \mu_e$ which allows a reduction of the transport problem to a single-electron-band case. From the $T = 2\,{\rm K}$ value $R_{\rm H} \approx -2.4 \times 10^{-9}\,{\rm m}^3/{\rm C}$, we would deduce $n_e = |R_{\rm H}e|^{-1} \approx 0.1/{\rm Co}$, which would correspond to a hole content $n_h \approx 0.43/{\rm Co}$. But in that case the anomalous decrease in magnitude of the Hall constant $R_{\rm H}$ with increasing T would correspond to a fourfold increase of the electron carrier content n_e up to 100 K. Also, this simple approach would imply the low-T anomalous increase of the electron mobility $\mu_e = |R_{\rm H}/\rho|$ shown in the insert of Fig. 4. The electron mobility $\mu_e \approx 330\,{\rm cm}^2/({\rm V\,s})$ at $T = 2\,{\rm K}$ would be much larger than the hole mobility mentioned above in the 0.77 phase.

In any case, it seems clear that high-mobility electrons are required to explain those data, but a serious explanation of these results can hardly be obtained without invoking a multiband behavior with sharp features at the Fermi level. This should not be surprising in view of the large paramagnetism which prevails at low temperatures in this phase, attributed to the Co kagome sublattice demonstrated by NMR data [11]. In most calculations done so far for kagome lattices flatbands are obtained. Our results, therefore, call for specific band structure calculations, taking into account the EC and the Na order.

B. Anomalous contribution to the Hall effect for $x = 0.77$

Let us compare now the AHE detected in the $x = 0.77$ AF phase to the observations done in various magnetic metals. In such cases an AHE has quite often been seen and is somewhat expected for ferromagnetic [37] but not for AF metals. It has, however, been seen in some specific AF compounds as discussed later. In some cases this AHE has been found to be dependent on the magnitude of the longitudinal current and named NLHE (for nonlinear HE) [38]. This does not apply to the present case, as we did find that here the AHE is independent of the current, as can be seen in the inset of Fig. 7 in Appendix B. Also, an AHE has been observed in AF metals in which the moments do not order with collinear orientations such as cubic Mn_3Ir [39,40]. Another type of AHE is detected even in zero field when a remanent magnetization remains after field cooling. It has been assigned to skyrmions either ordered or pinned by defects [41] and is often named the topological Hall effect (THE). We do see as well that a remanent magnetization is observed in our samples (see Appendix D). The fact that the negative Hall effect is nonlinear in field in our AF phase and changes at the spin flop or metamagnetic transition indicates that such possible origins for the AHE might be considered here and that domain walls might play a role as well. More refined experimental studies of the relation between $R_{\rm H}$ and the magnetic properties have to

be undertaken to determine whether the AHE is connected to local magnetization components which are not aligned along the c axis or might be related to residual disorder.

VI. SUMMARY

We have undertaken studies on various ordered Na phases and shown that the transport data is quite reproducible on our high-quality single-crystal samples. We disclose major pieces of evidence that the low-temperature transport properties are totally governed by the Co disproportionation associated with the Na ordering. Negative contributions to the Hall effect have been detected and indicate the occurrence of Fermi-surface reconstructions, similar to the case of cuprates in which a charge order was discovered, and subsequently was found to disrupt the SC order in some cases. The present results therefore reinforce the conclusion that in chemically doped layered materials the planar metallicity is quite generally strongly affected by the chemical order of the dopants, as has been suggested initially for the cuprates [42].

We have considered in some detail two phases with low-temperature negative Hall effect contributions. Our results evidence that these observations are related with important problems presently of great interest in the condensed matter community.

In the $x = 0.77$ AF metallic samples we find evidence that hole carriers apparently dominate the 2D charge transport, which seems to be a specific property of this phase. But in the vicinity of the AF state, a large negative contribution to the Hall effect is detected and found to be nonlinear in the applied field. We suggest that it has some analogy with the AHE observed in various AF metals. This might be connected with the fact that the Na-induced unit cell in the CoO_2 planes is noncentrosymmetric. Our results raises questions about the possible existence of noncollinear contributions to the magnetic order, e.g., skyrmions ordered or pinned by defects. Such fundamental questions are often highlighted in the community, particularly in view of possible spintronics applications in AF metals with high T_N values. The present results have led us to plan more detailed studies of the magnetotransport properties in this phase in high fields exceeding the metamagnetic transition.

On the contrary, the negative Hall effect is found to be linear in field for the $x = 2/3$ phase in a paramagnetic metallic regime where a disproportionated kagome structure of the CoO_2 planes has been established. The detected singular low-temperature variation of the Hall effect can be taken as evidence for a narrow energy feature in the band structure, such as a flatband, which is predicted by many calculations on kagome band structures [43]. While kagome lattices are heavily studied in half-filled insulating compounds in which a spin liquid state prevails [44], this $x = 2/3$ phase might be considered as a singular and original realization of a hole-doped metallic kagome structure. As QO have been detected initially in some cobaltate samples, we are presently engaged in such investigations in our cleaner samples. The attempt to get complementary information on the Fermi surface topology of this pure phase should stimulate specific band structure calculations, taking into account the electronic correlations, which are necessary to establish the disproportionated state [45]. The size of the unit cell might still be too large for the present state-of-the-art *ab initio* band structure calculations in correlated electron systems. Model calculations could, however, help to determine whether Weyl states and Berry phase effects could arise in such experimental conditions. In any case, our results raise some original questions about the interplay between topology and correlations in these layered materials.

ACKNOWLEDGMENTS

I.G. thanks F. Rullier-Albenque for her initial help in acquiring the experimental expertise required for transport experiments (she unfortunately passed away soon after the start of this project). We acknowledge frequent exchanges with L. Balicas and A. Subeidi, and thank V. Brouet, B. Gaulin and M. Leroux for their careful reading of the manuscript. The crystal growth, XRD, magnetic, and transport measurements were carried out at the Federal Center of Shared Facilities of Kazan Federal University. The work of I.R.M. was partially supported by the Russian Science Foundation (Project No. 19-12-00244). Travel between Kazan and Orsay has been financially supported by an "Investissement d'Avenir" allowance from the Labex PALM (No. ANR-10-LABX-0039-PALM).

APPENDIX A: SAMPLES AND MEASUREMENT TECHNIQUES

Single crystals of sodium cobaltates Na_xCoO_2 with $x \sim 0.8$ were grown using an optical floating zone technique. Subsequent electrochemical treatment was used in order to decrease sodium content and to obtain crystals with homogeneous sodium distribution. Details of the sample preparation techniques have been described elsewhere [17]. X-ray diffraction data allowed us to control the existence of a single value of the c-axis lattice parameter, which indicates the absence of phase mixing.

The longitudinal and transverse resistances R_{xx} and R_{xy} of the single crystals were measured by the van der Pauw method [46] and in some cases by the conventional six-contact method. Samples with an average size of 2×1 mm were prepared for the conventional resistivity measurements, and square-shaped crystals of average size 2×2 mm were prepared for measurements with the van der Pauw method. The sample thickness was less than 100 μm. The gold wires (50 μm diameter) used for the contacts were attached to the samples with silver paint. All resistance measurements were performed with the current in the *ab* plane of the crystal and magnetic field along the c axis.

The alternating current transport option (ACT) installed in the PPMS (PPMS-9, Quantum Design) was used for electrical resistance measurements in the 2–300 K temperature range in applied fields up to 9 T. Measurements of the AC electrical resistance at temperatures 0.1–3 K were performed in a dilution refrigerator BF-LD400 (BlueFors Cryogenics) using the same ACT electronics. The AC resistivity measurement frequency was 69 Hz, and the current magnitude was usually less than 0.5 mA at temperatures above 2 K and 0.1 mA for lower temperatures.

Hall voltage measurements on samples with six-contact were performed in positive and negative magnetic field (along

TABLE I. Measured resistivity at 300 and 2 K for the samples in Fig. 1. The residual resistivity ratio $RRR = \rho_1/\rho_2$ is given for the metallic samples.

x	$\rho_1(T = 300\,\mathrm{K})$ (mΩ cm)	$\rho_2(T = 2\,\mathrm{K})$ (mΩ cm)	RRR
0.5	0.79	113.5	
0.67	0.86	0.004	215
0.71	1.14	0.016	71
0.72	1.50	0.015	100
0.77	1.00	0.018	56

the c-axis direction) in order to subtract the contribution of the spurious longitudinal voltage due to contact misalignment. The Hall coefficient was defined as

$$R_{\mathrm{H}} = \frac{V_{xy}}{I_{xx}}\frac{d}{B} = R_{xy}\frac{d}{B},$$

where V_{xy} is the transverse voltage or Hall voltage, d the sample thickness, B the magnetic field, and R_{xy} is the transverse resistance or Hall resistance.

In Table I the resistivity values of the samples from Fig. 1 measured at 300 K and 2 K are given. The residual resistivity of metallic phases is much lower than the values shown in experiments published previously [20], and is found to be quite reproducible in our experiments. This confirms the high quality of the single crystals used.

APPENDIX B: REPRODUCIBILITY OF THE $x = 0.77$ TRANSPORT DATA

Resistivity and Hall coefficient measured for a series of $x = 0.77$ samples are displayed in Fig. 7. The resistivity data was found to be quite reproducible. The Hall effect measurements were taken using the van der Pauw technique after cooling the sample in zero field and then ramping up the field to 9 T. The Hall constant R_{H} was then measured for increasing temperatures in this 9-T applied field. The temperature dependences found are quite analogous for these distinct samples, with a large maximal negative values at about 14 K. The small differences in R_{H} magnitude cannot be assigned to sample geometrical factors; they might be due to slight differences in the remnant magnetization, as the actual local magnetization often has an influence on the AHE in AF metals. For a given sample (Cr13-19A Cr1) the data plotted in the inset of Fig. 7 were taken for longitudinal currents differing by one order of magnitude. This confirms that the Hall effect is linear in the longitudinal current.

APPENDIX C: FIELD VARIATION OF THE HALL EFFECT FOR $x = 0.77$

For an $x = 0.77$ sample the Hall effect data were taken with the standard six-contact method after cooling the sample to the lowest temperature in zero field. Then R_{xy} vs B curves were measured from the lowest to the highest temperatures – see Fig. 8. The data in this figure are qualitatively analogous to

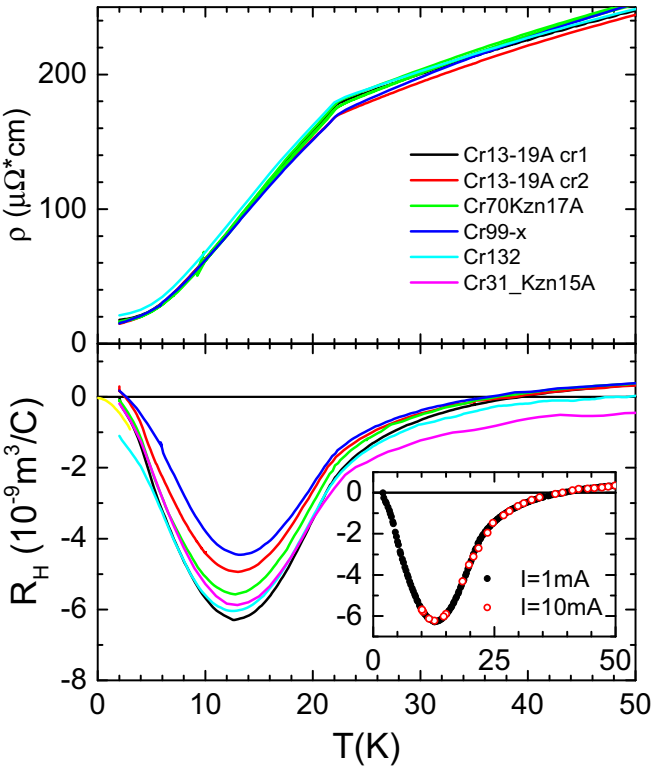

FIG. 7. Resistivity (upper frame) and Hall constant (lower frame) taken at low T on a series of 0.77 samples. Insert: R_{H} data taken for two longitudinal current values on one sample.

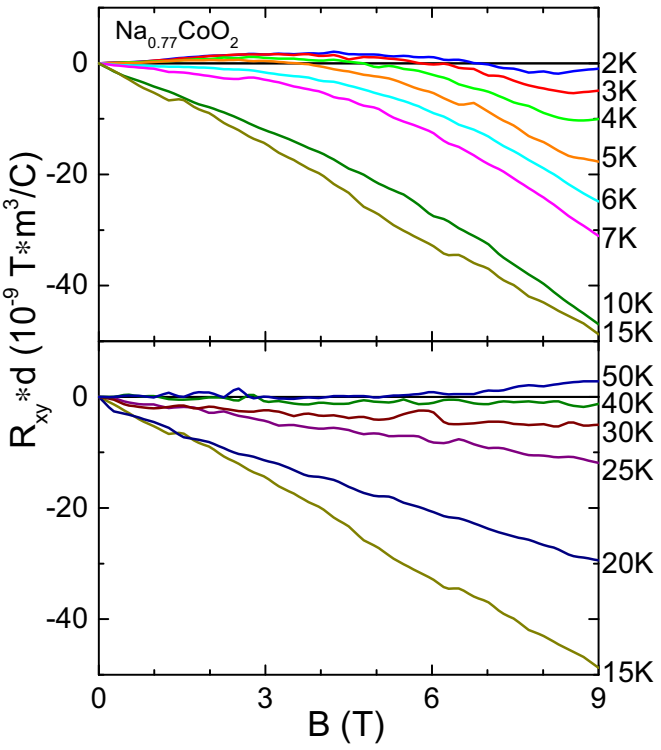

FIG. 8. Variation of the Hall constant with applied magnetic field B is plotted for increasing temperature, well below T_N in the upper frame and around and above T_N in the lower frame.

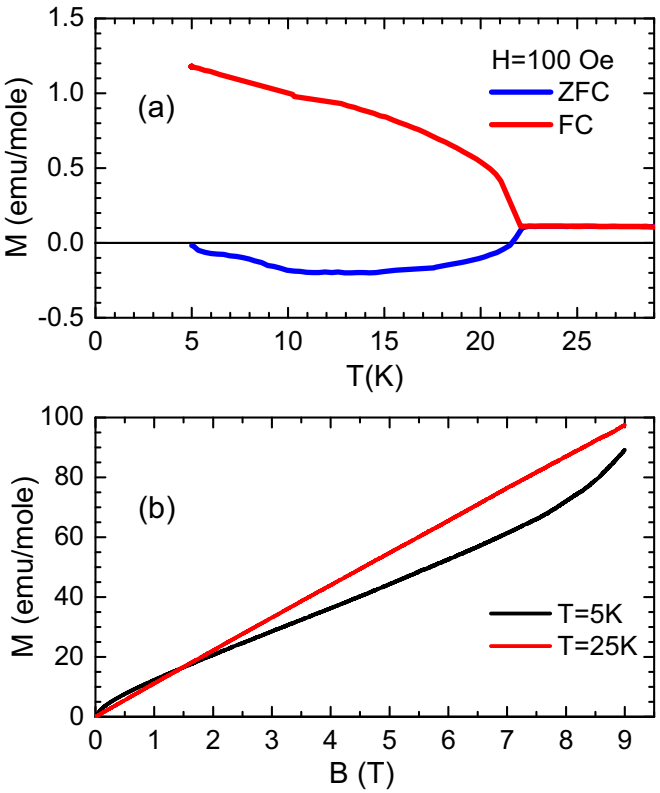

FIG. 9. (a) Magnetization measurement on a $x = 0.77$ phase sample after ZFC or FC. (b) Below T_N the field variation of the magnetization after ZFC is shown to display an increase at about 8 T which can be assigned to a spin flop or metamagnetic transition.

that of Fig. 3 obtained at lower T on a distinct sample with the van der Pauw technique. A linear behavior is recovered at about 15 K. The initial slope analysis of these results has been used to deduce the filled square data points plotted in the inset of Fig. 3.

APPENDIX D: MAGNETIC PROPERTIES OF THE $x = 0.77$ PHASE

The magnetic moment of $x = 0.77$ phase samples was measured using the vibrating sample magnetometer (VSM) of the PPMS (Quantum Design). The magnetic field was applied in the c direction of the crystal. Two types of temperature dependence of the magnetic moment were measured: the zero-field-cooling (ZFC) curve and the field-cooling curve (FC). First the magnetic field was set to zero value in oscillating mode to reduce the remnant magnetic field of the superconducting magnet; then the sample was cooled in zero magnetic field from T = 300 to 2 K, and the magnetic field was ramped to $H = 100$ Oe in the nonovershoot mode. Then the magnetic moment was measured while warming up (ZFC curve). The sample was then cooled back to $T = 2$ K without changing the applied magnetic field, and the magnetic moment was measured while warming up (FC curve). One can see in this experiment that a remnant magnetic moment is induced in the FC experiment below $T_N = 22$ K, as shown in Fig. 9(a).

After a ZFC the variation of the magnetization was measured in increasing magnetic field. For $T = 25$ K, that is, above T_N, the $M(B)$ curve of Fig. 9(b) is found linear. At $T = 5$ K in the AF state one can see a steplike increase for $B = 8$ T which can be associated with a spin flop of the local moments or a metamagnetic transition in the case of this metallic magnetic compound. A kink of the Hall constant is also detected for this field value below about 5 K, as can be seen in Figs. 3 and 8.

[1] P. A. Lee, N. Nagaosa, and X.-G. Wen, Doping a Mott insulator: Physics of high-temperature superconductivity, Rev. Mod. Phys. **78**, 17 (2006).

[2] K. Takada, H. Sakurai, E. Takayama-Muromachi, F. Izumi, R. A. Dilanian, and T. Sasaki, Superconductivity in two-dimensional CoO_2 layers, Nature (London) **422**, 53 (2003).

[3] J. Sugiyama, H. Itahara, J. H. Brewer, E. J. Ansaldo, T. Motohashi, M. Karppinen, and H. Yamauchi, Static magnetic order in $Na_{0.75}CoO_2$ detected by muon spin rotation and relaxation, Phys. Rev. B **67**, 214420 (2003).

[4] P. Mendels, D. Bono, J. Bobroff, G. Collin, D. Colson, N. Blanchard, H. Alloul, I. Mukhamedshin, F. Bert, A. Amato, and A. D. Hillier, Cascade of Bulk Magnetic Phase Transitions in Na_xCoO_2 as Studied by Muon Spin Rotation, Phys. Rev. Lett. **94**, 136403 (2005).

[5] K. S. Novoselov, A. K. Geim, S. V. Morozov, D. Jiang, Y. Zhang, S. V. Dubonos, I. V. Grigorieva, and A. A. Firsov, Electric field effect in atomically thin carbon films, Science **306**, 666 (2004).

[6] A. Castro Neto, N. M. R. Peres, K. S. Novoselov, and A. K. Geim, The electronic properties of graphene, Rev. Mod. Phys. **81**, 109 (2009).

[7] M. Z. Hasan and C. L. Kane, Topological insulators, Rev. Mod. Phys. **82**, 3045 (2010).

[8] N. P. Armitage, E. J. Mele, and A. Vishwanath, Weyl and Dirac semimetals in three-dimensional solids, Rev. Mod. Phys. **90**, 015001 (2018).

[9] I. R. Mukhamedshin and H. Alloul, Na order and Co charge disproportionation in Na_xCoO_2, Physica B: Condensed Matter **460**, 58 (2015).

[10] H. W. Zandbergen, M. L. Foo, Q. Xu, V. Kumar, and R. J. Cava, Sodium ion ordering in Na_xCoO_2: Electron diffraction study, Phys. Rev. B **70**, 024101 (2004).

[11] H. Alloul, I. R. Mukhamedshin, T. A. Platova, and A. V. Dooglav, Na ordering imprints a metallic kagome lattice onto the Co planes of $Na_2/3CoO_2$, Europhys. Lett. **85**, 47006 (2009).

[12] T. A. Platova, I. R. Mukhamedshin, H. Alloul, A. V. Dooglav, and G. Collin, Nuclear quadrupole resonance and x-ray investigation of the structure of $Na_2/3CoO_2$, Phys. Rev. B **80**, 224106 (2009).

[13] K.-W. Lee, J. Kunes, and W. E. Pickett, Charge disproportionation and spin ordering tendencies in Na_xCoO_2, Phys. Rev. B **70**, 045104 (2004).

[14] M. M. Korshunov, I. Eremin, A. Shorikov, V. I. Anisimov, M. Renner, and W. Brenig, Itinerant in-plane magnetic fluctuations and many-body correlations in Na_xCoO_2, Phys. Rev. B **75**, 094511 (2007).

[15] H.-B. Yang, Z.-H. Pan, A. K. P. Sekharan, T. Sato, S. Souma, T. Takahashi, R. Jin, B. C. Sales, D. Mandrus, A. V. Fedorov, Z. Wang, and H. Ding, Fermi Surface Evolution and Luttinger Theorem in Na_xCoO_2: A Systematic Photoemission Study, Phys. Rev. Lett. **95**, 146401 (2005).

[16] L. Balicas, J. G. Analytis, Y. J. Jo, K. Storr, H. Zandbergen, Y. Xin, N. E. Hussey, F. C. Chou, and P. A. Less, Shubnikov–de Haas Effect in the Metallic State of $Na_{0.3}CoO_2$, Phys. Rev. Lett. **97**, 126401 (2006).

[17] I. F. Gilmutdinov, I. R. Mukhamedshin, F. Rullier-Albenque, and H. Alloul, Synthesis of sodium cobaltate Na_xCoO_2 single crystals with controlled Na ordering, J. Phys. Chem. Solids. **121**, 145 (2018).

[18] H. Alloul, I. R. Mukhamedshin, A. V. Dooglav, Ya. V. Dmitriev, V.-C. Ciomaga, L. Pinsard-Gaudart, and G. Collin, 23Na NMR study of sodium order in Na_xCoO_2 with 22 K Neel temperature, Phys. Rev. B **85**, 134433 (2012).

[19] H. Alloul, I. R. Mukhamedshin, G. Collin, and N. Blanchard, Na atomic order, Co charge disproportionation and magnetism in Na_xCoO_2 for large Na content, Europhys. Lett. **82**, 17002 (2008).

[20] Maw Lin Foo, Yayu Wang, Satoshi Watauchi, H. W. Zandbergen, T. He, R. J. Cava, and N. P. Ong, Charge Ordering, Commensurability, and Metallicity in the Phase Diagram of the Layered Na_xCoO_2, Phys. Rev. Lett. **92**, 247001 (2004).

[21] G. Gašparović, R. A. Ott, J.-H. Cho, F. C. Chou, Y. Chu, J. W. Lynn, and Y. S. Lee, Neutron Scattering Study of Novel Magnetic Order in $Na_{0.5}CoO_2$, Phys. Rev. Lett. **96**, 046403 (2006).

[22] J. Bobroff, G. Lang, H. Alloul, N. Blanchard, and G. Collin, NMR Study of the Magnetic and Metal-Insulator Transitions in $Na_{0.5}CoO_2$: A Nesting Scenario, Phys. Rev. Lett. **96**, 107201 (2006).

[23] F. L. Ning, S. M. Golin, K. Ahilan, T. Imai, G. J. Shu, and F. C. Chou, ^{59}Co NMR Evidence for Charge Ordering Below $T_{CO} \sim 51$ K in $Na_{0.5}CoO_2$, Phys. Rev. Lett. **100**, 086405 (2008).

[24] G. Lang, J. Bobroff, H. Alloul, P. Mendels, N. Blanchard, and G. Collin, Evidence of a single nonmagnetic Co^{3+} state in the Na_1CoO_2 cobaltate, Phys. Rev. B **72**, 094404 (2005).

[25] C. deVaulx, M.-H.. Julien, C. Berthier, M. Horvatić, P. Bordet, V. Simonet, D. P. Chen, and C.T. Lin, Nonmagnetic Insulator State in Na_1CoO_2 and Phase Separation of Na Vacancies, Phys. Rev. Lett. **95**, 186405 (2005).

[26] D. LeBoeuf, N. Doiron-Leyraud, J. Levallois, R. Daou, J.-B. Bonnemaison, N. E. Hussey, L. Balicas, B. J. Ramshaw, R. Liang, D. A. Bonn, W. N. Hardy, S. Adachi, C. Proust, and L. Taillefer, Electron pockets in the Fermi surface of hole-doped high-Tc superconductors, Nature (London) **450**, 533 (2007).

[27] N. Doiron-Leyraud, C. Proust, D. LeBoeuf, J. Levallois, J. B. Bonnemaison, R. Liang, D. A. Bonn, W. N. Hardy, and L. Taillefer, Quantum oscillations and the Fermi surface in an underdoped high-Tc superconductor, Nature (London) **447**, 565 (2007).

[28] Y. Wang, N. S. Rogado, R. J. Cava, and N. P. Ong, Anomalous high-temperature Hall effect on the triangular lattice in Na_xCoO_2, arXiv:cond-mat/0305455.

[29] W. Koshibae, A. Oguri, and S. Maekawa, Anomalous high-temperature Hall effect on the triangular lattice in Na_xCoO_2, Phys. Rev. B **75**, 205115 (2007).

[30] G. León, C. Berthod, T. Giamarchi, and A. J. Millis. Hall effect on the triangular lattice. Phys. Rev. B **78**, 085105 (2008).

[31] F. Rullier-Albenque, D. Colson, A. Forget, and H. Alloul, Hall Effect and Resistivity Study of the Magnetic Transition, Carrier Content and Fermi Liquid Behavior in $Ba(Fe_{1-x}Co_x)2As_2$, Phys. Rev. Lett. **103**, 057001 (2009).

[32] V. Brouet, P.-H. Lin, Y. Texier, J. Bobroff, A. Taleb-Ibrahimi, P. Le Fèvre, F. Bertran, M. Casula, P. Werner, S. Biermann, F. Rullier-Albenque, A. Forget, and D. Colson, Large Temperature Dependence of the Number of Carriers in Co-Doped $BaFe_2As_2$, Phys. Rev. Lett. **110**, 167002 (2013).

[33] S. P. Bayrakci, I. Mirebeau, P. Bourges, Y. Sidis, M. Enderle, J. Mesot, D. P. Chen, C. T. Lin, and B. Keimer, Magnetic Ordering and Spin Waves in $Na_{0.82}CoO_2$, Phys. Rev. Lett. **94**, 157205 (2005).

[34] I. R. Mukhamedshin, H. Alloul, G. Collin, and N. Blanchard, 23Na NMR Evidence for Charge Order and Anomalous Magnetism in Na_xCoO_2, Phys. Rev. Lett. **93**, 167601 (2004).

[35] F. Rullier-Albenque, Influence of the electronic structure on the transport properties of iron pnictides, C. R. Phys. **17**, 164 (2015).

[36] I. R. Mukhamedshin, A. V. Dooglav, S. A. Krivenko, and H. Alloul, Evolution of Co charge disproportionation with Na order in Na_xCoO_2, Phys. Rev. B **90**, 115151 (2014).

[37] N. Nagaosa, J. Sinova, S. Onoda, A. MacDonald, and N. P. Ong, Anomalous Hall effect, Rev. Mod. Phys. **82**, 1539 (2010).

[38] I. Sodemann and L. Fu, Quantum Nonlinear Hall Effect Induced by Berry Curvature Dipole in Time-Reversal Invariant Materials, Phys. Rev. Lett. **115**, 216806 (2015).

[39] H. Chen, Q. Niu, and A. H. MacDonald, Anomalous Hall Effect Arising from Noncollinear Antiferromagnetism, Phys. Rev. Lett. **112**, 017205 (2014).

[40] J. Kubler and C. Felser, Non-collinear antiferromagnets and the anomalous Hall effect, Europhys. Lett. **108**, 67001 (2014).

[41] B. S. Kim, Skyrmions and Hall transport, J. Phys.: Condens. Matter. **31**, 383001 (2019).

[42] H. Alloul, What is the simplest model which captures the basic experimental facts of the physics of underdoped cuprates?, C. R. Phys. **15**, 519 (2014).

[43] I. Mazin, H. O. Jeschke, F. Lechermann, H. Lee, M. Fink, R. Thomale, and R. Valentí, Theoretical prediction of a strongly correlated Dirac metal, Nat. Commun. **5**, 4261 (2014).

[44] P. Khuntia, M. Velazquez, Q. Barthélemy, F. Bert, E. Kermarrec, A. Legros, B. Bernu, L. Messio, A. Zorko, and P. Mendels, Gapless ground state in the archetypal quantum kagome antiferromagnet $ZnCu_3(OH)_6Cl_2$, Nat. Phys. **16**, 469 (2020).

[45] Y. V. Lysogorskiy, S. A. Krivenko, I. R. Mukhamedshin, O. V. Nedopekin, and D. A. Tayurskii, Origin of the electron disproportionation in the metallic sodium cobaltates, Phys. Rev. B **94**, 205138 (2016).

[46] L. J. van der Pauw, A method of measuring specific resistivity and Hall effect of discs of arbitrary shape, Philips Res. Rep. **13**, 1 (1958).